Int. J. Heat Mass Transfer. Vol. 15, pp. 1709–1717. Pergamon Press 1972. Printed in Great Britain

CONVECTIVE HEAT TRANSFER TO WATER CONTAINING BUBBLES: ENHANCEMENT NOT DEPENDENT ON THERMOCAPILLARITY

D. B. R. KENNING and Y. S. KAO*

Department of Engineering Science, Oxford University, Parks Road, Oxford, England

(*Received* 6 *September* 1971 *and in revised form* 15 *December* 1971)

Abstract—Upstream injection of small gas bubbles causes increases of up to 50 per cent in heat-transfer coefficient for water flowing upward in a channel of rectangular cross-section. The increase depends on gas flow rate and liquid phase Reynolds number but not on heat flux, indicating that thermocapillary flows do not contribute to the heat transfer. A possible mechanism for the increase is secondary flow production by the interaction of bubbles with the shear flow near the wall.

NOMENCLATURE

A, wall area round bubble; channel aspect ratio b/d, equation (1);
A_0, projected area of bubble, $= \pi a^2$
a, bubble radius;
b, channel width, heated side;
d, channel depth, normal to heated side;
F, function of liquid Reynolds number Re_l equation (7);
G, function of dimensionless area z, equation (7);
h, mean heat-transfer coefficient over entire surface;
h_t, heat-transfer coefficient for turbulent liquid flow without gas;
h_z, local heat-transfer coefficient at perimeter of area z;
$\bar{h}_z$, mean heat-transfer coefficient over area z;
j, volumetric flux, volumetric flow rate divided by channel cross-sectional area;
N, number of bubbles per unit area of heated surface;
Nu, Nusselt number;
Pr, Prandtl number;
Re, Reynolds number;
S, fraction of heated surface covered by bubbles;
v, mean velocity;
v_{gl}, bubble slip velocity;
z, dimensionless area round bubble, $= A/\pi a^2$;
α, void fraction;
μ_r, ratio of wall to bulk viscosity.

Subscript
g, gas;
l, liquid.

* Present address, Department of Mechanical Engineering, University of British Columbia.

1. INTRODUCTION

IT HAS been suggested that local thermocapillary flows round entrained vapour bubbles could make a major contribution to the overall rate of heat transfer in subcooled flow boiling [1]. This hypothesis has been tested by measuring the rate of forced-convection heat transfer to water containing small bubbles of nitrogen. Any thermocapillary effects should be stronger for gas bubbles with a near-adiabatic boundary condition at the liquid–gas interface than for vapour bubbles, for which internal evaporation–condensation processes reduce the interfacial

temperature (and therefore surface tension) gradients. The effects should also be more pronounced at high heat flux than at low flux, again because of the larger temperature gradients available to drive thermocapillary flows. It was found that improvements in heat-transfer coefficient of up to 50 per cent occurred in the presence of quite small quantities of gas (volumetric flow ratios of up to 0·07 with the gas present as bubbles of nominal diameter 1·5 mm), but that the improvements were independent of heat flux over the range 20–300 kW/m.^{2} This linear dependence of heat flux on the temperature difference between the wall and the bulk for given rates of gas and liquid flow suggests that thermocapillary flows made negligible contribution to the heat transfer process.

Flows induced by surface-tension gradients are very sensitive to the presence of surface-active impurities. The mechanism of flow suppression by impurities has been discussed in detail elsewhere for the thermocapillary flow round a hemispherical bubble on a heated wall [2]. In the present experiments the surface tension of the water in the apparatus remained within 0·2 dynes/cm of the value for pure water throughout the duration of the tests. This was achieved only by the use of triple-distilled water and rigorous cleaning of the apparatus, which was designed so that the only materials in contact with the water were stainless steel and polytetrafluoroethylene (ptfe). Because of these precautions the level of surface-active contamination was probably lower than would occur in most systems containing water. In boiling systems with net evaporation surface-active impurities become concentrated in the boiling region [3]; the distribution of surfactant in a system employing only subcooled boiling might be more uniform. While extrapolation from the flow studied in [2] suggests that thermocapillary flows should not have been greatly affected by the small amount of contamination for the sizes of bubbles and heat fluxes used in these experiments, this expectation could only be confirmed by a detailed analysis of the flow near an entrained bubble and this has not been attempted. In previous measurements of heat-transfer coefficients to liquids containing bubbles, summarized by Kudirka [4], no special precautions to exclude surfactants were reported nor were heat-flux dependent effects specifically sought.

2. EXPERIMENTAL EQUIPMENT

Heat transfer rates were measured for water flowing upwards through a vertical channel of rectangular cross-section 4·8 mm × 12·7 mm × 450 mm long with a smooth transition at entry and exit to 32 mm bore tubing. The external circuit consisted of a water-cooled heat exchanger,

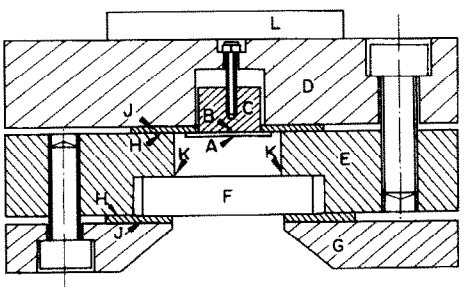

A Test surface, stainless steel
B Silicone adhesive
C Sindanyo strip
D Sindanyo back plate
E Test section body, stainless steel
F Glass window
G Window clamp
H Unsintered ptfe tape, 4 layers
J Silicone rubber
K ptfe spray
L Guard heater

FIG. 1. Test section construction.

circulating pump, variable-area flow meters, preheating section and a bypass to a degassing/pressurizing tank. The channel was heated on one side over an area 11 mm wide, 300 mm long. The form of construction shown in Fig. 1 was adopted to combine the noncontaminating properties of ptfe with the sealing properties of silicone rubber. The gas bubble injector was situated at the leading edge of the heated section and is shown in Fig. 2. It produced five equi-spaced streams of bubbles at a distance of 0·25

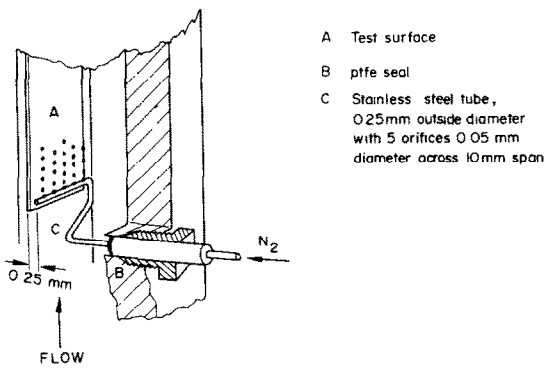

FIG. 2. Gas bubble injector.

mm from the heated surface. The mean bubble diameter was 1·5 mm. The injector was supplied with oil-free nitrogen through two filters, a precision pressure regulator and a variable-area flow meter. The test surface of the channel was of 0·25 mm thick stainless steel, heated by direct current from a modified 18 kVA welding rectifier through a precision resistance for current measurement and a water-cooled resistance for fine adjustment.

Before each day's run the water in the apparatus was degassed by boiling under vacuum for 1 h in the degassing/pressurizing tank with a low flow rate between the tank and the primary circuit. This was necessary both to avoid corrosion of the test surface by dissolved oxygen and also to prevent gas bubble nucleation on the hot surface. In order to prevent electrolytic bubble formation the unheated stainless steel body of the test section was sprayed with ptfe (Rocal I.F.L. Lubricant), giving a leakage resistance of 100 kΩ between the body and the test surface prior to earthing the body and power supply anode. With these precautions, there was no detectable corrosion of the test surface over a period of several weeks and no electrolysis could be detected photographically when the maximum power was supplied to the surface.

Bulk water temperatures at inlet and outlet to the test section were measured by copper–constantan thermocouples in pockets. The fluid enthalpy rise agreed with the electrical power measurements to within 5 per cent. Wall temperatures were measured by ten copper–constantan, glass-insulated thermocouples held against the rear surface of the heated strip by springs. Mica discs 0·05 mm thick were placed between the thermocouple junctions and the surface to prevent electrical pickup. Auxiliary thermocouples were used to measure the temperature gradient across the sindanyo backing strip of the heated surface and three electrical guard heaters on the rear of the test section were adjusted to minimize these gradients. With allowance for the temperature difference across the thickness of the heated surface, wall temperatures were estimated to be accurate to $\pm$ 0·5 C.

3. MEASUREMENTS

(i) *Without gas injection*

Experiments were performed at Reynolds numbers in the range 10^4–6×10^4, based on the mean hydraulic diameter of the channel. The heat-transfer coefficient reached a steady value 150 mm from the leading edge of the heated strip, but over the last 30 mm of the strip the wall temperature showed an apparent decrease which could be reduced but not eliminated by adjustment of the last guard heater. Similar behaviour has been reported by other experimenters [1, 5]. Over the central region of the channel the measured heat-transfer coefficients, shown in Fig. 3, were in close agreement with

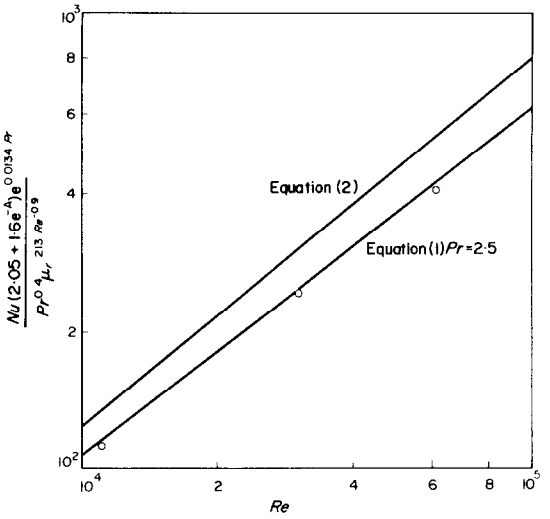

FIG. 3. Heat-transfer data without gas injection.

the correlation proposed by James *et al.* [6] for fully-developed turbulent flow,

$$\frac{Nu\,(2{\cdot}05 + 1{\cdot}6\,e^{-A})\,e^{0{\cdot}0134\,Pr}}{Pr^{0{\cdot}4}\,\mu_r^{2{\cdot}13\,Re^{-0{\cdot}9}}} = 0{\cdot}104\,Re^{0{\cdot}0016\,Pr + 0{\cdot}75} \qquad (1)$$

with fluid properties evaluated at the local bulk temperature. Measurements in this central region were used in the subsequent comparative measurements of the effects of gas injection.

For the configuration used in these experiments the older (and more convenient) Sieder–Tate correlation,

$$Nu = 0{\cdot}027\quad Re^{0{\cdot}8}Pr^{0{\cdot}33}\mu_r^{-0{\cdot}14} \qquad (2)$$

over-estimated the heat-transfer coefficients by 10–25 per cent, Fig. 3.

(ii) *With gas injection*

Measurements were made at three water flow rates (volumetric flux $j_l = 0{\cdot}6$, 1·2 and 1·8 m/s) and three gas flow rates ($j_g = 0{\cdot}11$, 0·022 and 0·044 m/s). Heat flux and measured temperature difference are plotted logarithmically in Fig. 4 for each combination of flow rates. The lines run

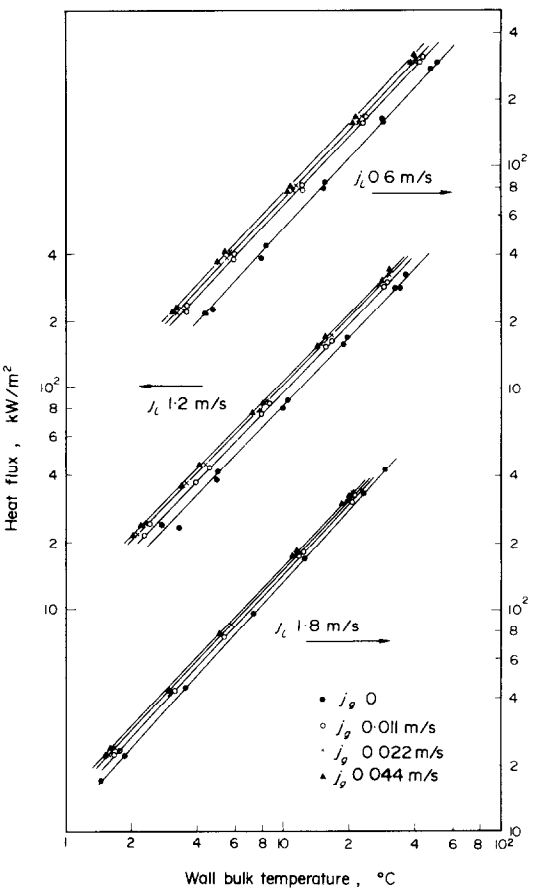

FIG. 4. Heat-transfer data with gas injection.

parallel to those for zero gas flow, the slight departures from a slope of unity following the effects of temperature-dependent properties given by equation (1). Measurements at different bulk inlet temperatures confirmed that these small variations in heat-transfer coefficient depended on temperature and not on heat flux.

Gas injection was most effective in improving heat transfer at low liquid flow rates, Fig. 5. For a given liquid flow, increases in gas flow rate beyond the minimum flow used produced rather small further improvements in heat-transfer coefficient. Irregular bubble production at low gas flow rates with the existing design of

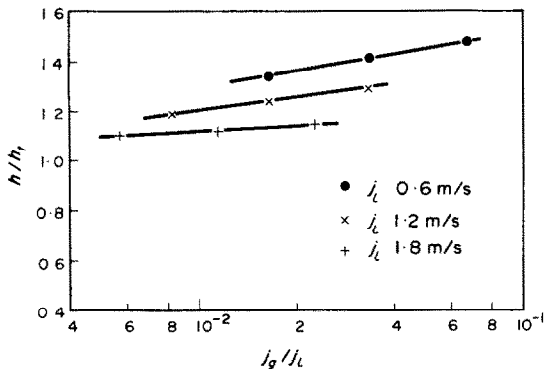

FIG. 5. Increase in heat-transfer coefficient due to gas injection.

gas injector prevented investigation of still smaller flow rates.

In addition to the thermal measurements, during a few runs the flow was photographed using a single-flash light source of 2 μs duration. By using oblique lighting the relative positions of a bubble and its shadow could be used to estimate the gap between the bubble and the wall. Typically this was about 0·05 mm, i.e. so small that local bubble deformation would determine its precise value. Most of the bubbles remained close to the wall (having been injected at a distance of 0·25 mm), irrespective of whether the test surface was heated or not. There was no evidence of significant bubble coalescence.

4. ANALYSIS AND DISCUSSION

The presence of gas bubbles may affect heat transfer between the wall and the turbulent liquid phase by the following mechanisms.

(i) Increased turbulence due to the increased liquid velocity.
(ii) Thermocapillary flows near the bubbles.
(iii) Disturbance of the wall region by the flow patterns generated by relative motion of the gas and liquid phases.

Mechanism (i) can be discounted in the present study, where the increases in liquid mean velocity due to gas injection were of order 5 per cent, insufficient to produce the measured improvements in heat-transfer coefficient of up to 50 per cent. Thermocapillary flows, by analogy with the flow near a hemispherical bubble [2], might be expected to influence wall-liquid heat transfer over a rather localized region of area not more than twice the projected bubble area. Fig. 6; the generation of motion by shear

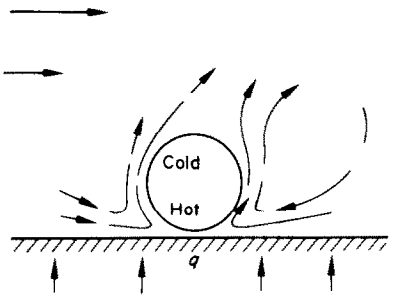

FIG. 6. Postulated thermocapillary flow near an entrained bubble.

stresses at the bubble surface causes liquid flow nearly parallel to the wall on the hot "supply" side, developing into a jet normal to the wall only on the cold "delivery" side of the bubble. By contrast, the flow due to slip round a bubble could affect a much larger region of the wall, particularly if it leads to a disturbed wake. The independence of heat-transfer coefficient and heat flux has already been cited as evidence that thermocapillary flows do not affect the heat transfer significantly. Confirmation will now be sought by examining the extent of the wall region over which heat transfer is influenced by an individual bubble.

Since the flow was photographed only on a few runs, the bubble concentration per unit area of heated wall, N, must be deduced from the gas and liquid flow rates by assuming a suitable value for the bubble slip velocity, v_{gl}. Fortunately a precise value is not necessary; for the conditions of these experiments a 100 per cent error in v_{gl} produces at worst a 20 per cent error in void fraction. The free rise velocity of a bubble 1·5 mm dia. is about 0·25 m/s but would be reduced by the presence of the channel walls [7],

say to 0·15 m/s ± 50 per cent. Any effects of the liquid velocity v_l and of the presence of other bubbles are ignored. The void fraction α is given by

$$\alpha = \frac{j_g}{v_g} = \frac{j_g}{v_l + v_{gl}}. \tag{3}$$

For the low values of α in these experiments

$$v_l = \frac{j_l}{1 - \alpha} \approx j_l. \tag{4}$$

Assuming that all bubbles remain close to the heated wall,

$$N = \frac{3dj_g}{4\pi a^3(j_l + v_{gl})}, \tag{5}$$

where a is bubble radius and d the channel depth normal to the heated surface. Taking the projected area per bubble as πa^2, the fraction S of the surface covered by bubbles is

$$S = \frac{3dj_g}{4a(j_l + v_{gl})}. \tag{6}$$

The following simple model is adopted for heat transfer to a liquid flow containing a small number of bubbles of uniform (and constant) size. Near each bubble the normal heat transfer to the turbulent liquid in the absence of bubbles, h_t, is increased over an area A. It will be assumed that the variations in heat-transfer coefficient can be represented by an expression of the form

$$\frac{h_z}{h_t} = F(Re_l) \cdot G(z) \tag{7}$$

where z is area A made dimensionless with respect to the bubble projected area πa^2,

$$z = \frac{A}{\pi a^2}, \tag{8}$$

and h_z is the value of the heat-transfer coefficient at the perimeter of the area. $\bar{h}_z$ is the mean value of the heat-transfer coefficient within this perimeter. Thus it is assumed that the magnitude of the increase in heat-transfer coefficient h_z/h_t depends on the liquid Reynolds number, Re_l, but the shape of its distribution does not. At low bubble concentrations h_z/h_t should approach 1 at the edge of the area of influence of each bubble, Fig. 7a. When the areas of influence overlap, Fig. 7b, it is assumed that values of h_z in the non-overlapping regions are unaltered. For a given bubble size the amount of overlap and therefore the value of $\bar{h}_z/h_t$ applying over the entire surface depends on the fractional surface coverage, S. At values of S low enough for there to be no overlap the mean (i.e. measured) heat-transfer coefficient h should increase linearly with S. Measured values of $(h/h_t - 1)$ are plotted against calculated values of S in Fig. 8. By choice of suitable values for $F(Re_l)$ in equation (7), namely

$$F_2/F_3 = 1{\cdot}8, \qquad F_1/F_3 = 2{\cdot}7 \tag{9}$$

where subscripts 1, 2, 3 denote liquid velocities

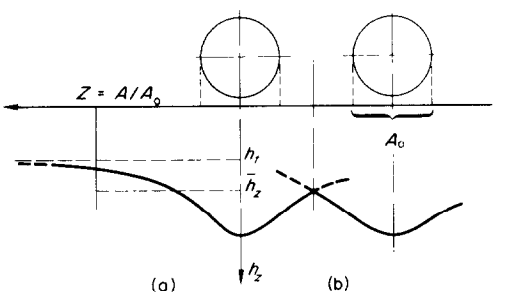

FIG. 7. Area of influence of a bubble (a) in isolation (b) with overlap.

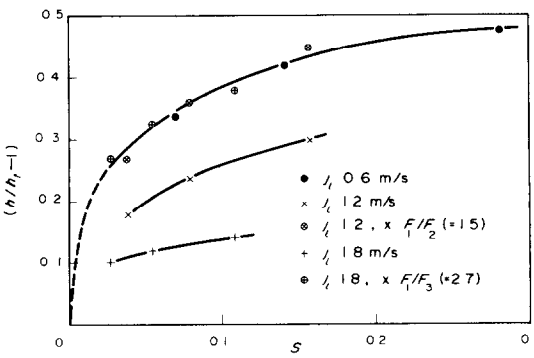

FIG. 8. Variation of heat-transfer coefficient with fraction of wall covered by bubbles.

of 0·6, 1·2 and 1·8 m/s respectively, the measurements can be represented by a single curve, in accordance with the assumed model. Any region of linear variation of $(h/h_t - 1)$ with S, if it exists at all, is restricted to $S < 0{\cdot}025$. This implies that the area of influence of a bubble is at least 40 times its projected area, much greater than would be expected for thermocapillary effects and indeed larger than would be expected from the pattern of uniform flow past a sphere at Reynolds numbers of about 400 (based on slip velocity) for which the separated wake region extends only 1–2 diameters downstream. However, Schlichting [8] measured significant secondary flows in a boundary-layer flow 10 diameters downstream of an array of spheres on a wall; Seban and Caldwell [9], investigating turbulent boundary-layer flow past a single sphere on a wall, found increases in heat transfer coefficient in a wake 4 diameters wide and extending more than 40 diameters downstream, Fig. 9. This

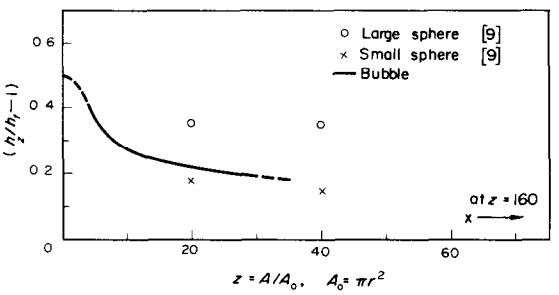

FIG. 9. Local variations in heat-transfer coefficient near a stationary solid sphere [9] and a moving bubble.

effect far beyond the reattachment point of the separated flow behind the sphere is presumably due to the generation of vortices with streamwise axes, as described in [3] for laminar flow conditions. It seems possible that interaction between a moving bubble and the shear flow near the wall would cause similar secondary flows which persist for long distances downstream. Further information about the local variations in heat-transfer coefficient near a bubble can be deduced from the overall coefficient measurements in the region of overlap, using the relations derived in the Appendix

$$h_z = \bar{h}_z + z\frac{d\bar{h}_z}{dz} = h - S\frac{dh}{dS}. \qquad (10)$$

Local values of $(h_z/h_t - 1)$ thus deduced from Fig. 8 are shown in Fig. 9. The slow rate of decay of the bubble disturbance at $z > 20$ is similar to that behind a sphere from (9), despite the relatively high sphere Reynolds numbers of $1{\cdot}3 \times 10^4$ and 4×10^4 in the latter study. Differences in behaviour at small z are to be expected in view of the different boundary conditions. The increase in h_z close to the bubble could be due to local hydrodynamic interaction with the wall, thermocapillary flow or simply inapplicability of the analytical model as bubbles become close-packed. Thus the study of the area of influence of bubbles has added nothing to the previously discussed evidence concerning the role of thermocapillary effects but has shown that, whatever the details of the flow very close to the bubble, the main effect on heat transfer at low void fractions is due to long-lived secondary flows at relatively large distances from the bubble. Extrapolation of the empirically chosen values of $F(Re_l)$, Fig. 10, suggests that the effect

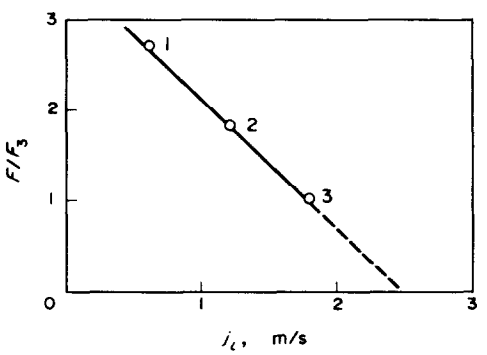

FIG. 10. Effect of liquid velocity on heat-transfer augmentation by gas bubbles.

of bubbles on heat transfer would become negligible at liquid velocities $v_l > 2{\cdot}5$ m/s, i.e. when the bubble slip velocity v_{gl} of 0·15 m/s

becomes small compared to the largest turbulent fluctuations in liquid velocity of order $0{\cdot}1\, v_l$.

The generation of secondary vortices would be effective only for bubbles in the high shear wall region. Although there is no evidence for a direct contribution to heat transfer by thermocapillarity, under some circumstances it might exert an indirect influence by modifying the distribution of bubbles. In the present experiments, with bubbles injected close to the wall, bubble trajectories were not noticeably affected by heat flux but the tendency for vapour bubbles in boiling to remain close to the wall [10] might be due to thermocapillarity.

5. CONCLUSIONS

For the conditions of these experiments the presence of small gas bubbles can increase convective heat transfer by up to 50 per cent. The increase is not dependent on heat flux, ruling out thermocapillarity as the mechanism, so that entrained vapour bubbles should cause a similar (but no greater) effect. Flow boiling correlations which consider separate contributions by boiling and single phase heat transfer, e.g. Chen [11], should allow for the enhancement of the single phase coefficient by small bubbles under slightly subcooled or bulk boiling conditions.

A possible mechanism for the improvement in heat transfer is the production of secondary flows by the motion of the bubbles in the shear flow near the wall. Vortices with streamwise axes could persist over a long wake region behind each bubble, explaining the increase in heat-transfer coefficient at very low bubble concentrations: 50 per cent of the increase is produced at less than 2·5 per cent coverage of the wall by bubbles. If this is indeed the mechanism then bubbles in the central region of the flow would be ineffective and the experimental results as presented in Fig. 5 should not be applied to a flow geometry with a different distribution of bubbles across the channel. Figure 8 should still apply, however, with a suitable definition of S in terms of the bubbles lying within the high velocity gradient region of the flow. The effect of bubbles on heat transfer is negligible when the bubble slip velocity is less than about 6 per cent of the mean velocity of the turbulent liquid flow. The effect of bubble size was not investigated.

The injection of small gas bubbles at the inlet of low-velocity turbulent flow in a vertical channel appears to be a feasible means of augmenting heat transfer to a liquid. Although an unlikely choice at the initial design stage, it could be a simple way of uprating existing equipment. Where simultaneous heat transfer and chemical reaction between a gas and a liquid are required this method is clearly of interest.

ACKNOWLEDGEMENT

This work was supported by Babcock and Wilcox (Operations) Ltd.

REFERENCES

1. W. T. Brown, Ph.D. Thesis, Department of Mechanical Engineering, Massachusetts Institute of Technology (1967).
2. Y. S. Kao, D.Phil. Thesis, Oxford University (1970).
3. D. B. R. Kenning and M. G. Cooper, Flow patterns near nuclei and the initiation of boiling during forced convection heat transfer. *Proc. Inst. Mech. Engrs* **180** (Part 3c), 112 (1965–66).
4. A. A. Kudirka, Two-phase heat transfer with gas injection through a porous boundary surface, Argonne National Laboratory Report ANL-6862 (1964).
5. W. C. Elrod, J. A. Clark, E. R. Lady and H. Merte, Boiling heat transfer data at low heat flux, *J. Heat Transfer* **89C**, 235 (1967).
6. D. D. James, B. W. Martin and D. G. Martin, Forced convection heat transfer in asymmetrically heated ducts of rectangular cross-section, Proc. 3rd Int. Heat Transfer Conf., Vol. I, p. 85 (1966).
7. G. B. Wallis, *One-Dimensional Two-Phase Flow*. McGraw-Hill, New York (1969).
8. H. Schlichting, *Boundary Layer Theory*. McGraw-Hill, New York (1955).
9. R. A. Seban and G. L. Caldwell, The effect of a spherical protuberance on the local heat transfer to a turbulent boundary layer, *J. Heat Transfer* **90C**, 408 (1968).
10. L. M. Jiji and J. A. Clark, Bubble boundary layer and temperature profiles for forced convection boiling in channel flow, *J. Heat Transfer* **86C**, 50 (1964).
11. J. C. Chen, Correlation for boiling heat transfer to saturated fluids in convective flow, *Ind. Engng Chem. Proc. Des. Dev.* **5**, 322 (1966).

APPENDIX

$$\bar{h}_z = \frac{1}{z}\int_0^z h_z \, dz. \tag{A.1}$$

$$\bar{h}_{z+dz} = \frac{1}{z+dz}(\bar{h}_z z + h_z \, dz), \tag{A.2}$$

$$= \bar{h}_z + (h_z - \bar{h}_z)\frac{dz}{z} + 0\left[\left(\frac{dz}{z}\right)\right]^2 \tag{A.3}$$

$$\therefore h_z = \bar{h}_z + z\frac{d\bar{h}_z}{dz}. \tag{A.4}$$

When regions of influence overlap

$$z = \frac{1}{S}, \qquad \bar{h}_z = h; \tag{A.5}$$

$$h_z = h - s\frac{dh}{dS} \tag{A.6}$$

and h_z can then be found from Fig. 8.

TRANSFERT THERMIQUE PAR CONVECTION DANS L'EAU CONTENANT DES BULLES: ACCROISSEMENT INDEPENDANT DE LA THERMOCAPILLARITE

Résumé—Une injection en amont de petites bulles gazeuses provoque un accroissement atteignant 50 pour cent du coefficient de transfert thermique pour de l'eau qui s'écoule dans un canal à section rectangulaire. L'accroissement dépend du débit de gaz et du nombre de Reynolds de la phase liquide mais pas du flux thermique ce qui indique que les écoulements thermocapillaires ne contribuent pas au transfert de chaleur. Une mécanisme possible de l'augmentation serait la création d'un écoulement secondaire par interaction des bulles avec l'écoulement de cisaillement près de la paroi.

KONVEKTIVE WÄRMEÜBERTRAGUNG AN BLASENHALTIGES WASSER. VERBESSERUNG UNABHÄNGIG VON DER THERMOKAPILLARITÄT

Zusammenfassung—Die Injektion kleiner Gasblasen stromaufwärts verursacht einen bis zu 50-prozentigen Anstieg des Wärmeübertragungskoeffizienten für Wasser, das in einem Kanal mit rechwinkligem Querschnitt fliesst. Dieser Anstieg hängt ab von der Grösse des Gaszuflusses und der Reynolds-Zahl der flüssigen Phase, nicht aber von der Wärmestromdichte. Das bed ıtet, dass Thermokapillarströmungen zur Wärmeübertragung nicht beitragen. Ein möglicher Mechanismus für den Anstieg ist die Erzeugung eines Sekundärstromes durch die Wechselwirkung der Blasen mit der Scherströmung nahe der Wand.

КОНВЕКТИВНЫЙ ТЕПЛООБМЕН В ВОДЕ, СОДЕРЖАЩЕЙ ПУЗЫРЬКИ: УВЕЛИЧЕНИЕ КОЭФФИЦИЕНТА ТЕПЛООБМЕНА, НЕЗАВИСИМОЕ ОТ ТЕРМОДИФФУЗИИ

Аннотация—Ввод небольших пузырьков газа по течению восходящего потока воды в канале прямоугольного сечения вызывает увеличение коэффициента теплообмена до 50%. Это увеличение зависит от расхода газа и числа Рейнольдса жидкой фазы и не зависит от теплового потока, указывая на то, что термодиффузионные потоки не влияют на теплообмен. Возможный механизм, объясняющий этот рост, заключается в возникновении вторичного течения, вызванного взаимодействием пузырьков со сдвиговым потоком вблизи стенки.